

Continuous reactor system of monosized colloidal particles

TAKASHI OGIHARA, MANABU IIZUKA, TERUAKI YANAGAWA, NOBUO OGATA, KOKICHI YOSHIDA

Department of Materials Science and Engineering, Fukui University, 9-1, Bunkyo 3, Fukui-shi, Fukui-ken, 910, Japan

A reactor system, which continuously hydrolysed the metal alkoxide in an alcohol solution, was designed using an electromagnetic stirrer and an ageing tube. Several monosized colloidal particles were produced by this reactor system, which had high reproducibility and reliability for long-term production. The relation between powder characteristics and experimental parameters such as reagent concentration, mixing rate, ageing time, temperature, was investigated. These parameters had an effect on the particle size, size distribution, morphology and state of agglomeration. It is possible to control the particle size to between 0.1 and 1.0 μm by varying the experimental conditions. A narrower size distribution of powders was obtained by using an electromagnetic stirrer with greater flow rate. Physical and chemical properties of monosized colloidal particles obtained by this reactor were comparable to those of monosized colloidal particles obtained by the batch process.

1. Introduction

Recently, ceramic powders with fine, narrow size distribution and nonagglomeration have been produced by chemical synthesis using organometallic precursors [1-3]. Hydrolysis of metal alkoxide is well known as a fine-powder preparation technique. Sol-gel processing involves the alkoxide route widely used for ceramic industrial application such as fibre coating and thin films [4-9]. Metal alkoxide reacts with water to form a hydrolysis species and then condenses to a polymeric compound. The size, size distribution, morphology and agglomeration of particles were affected by the concentration of alkoxide, the ratio of starting reagents (alkoxide and water), the nature of metal alkoxide and solvent and pH in the hydrolysis. The alkyl type of alkoxide was influenced by the rate of hydrolysis and condensation. As the alkyl group of the alkoxide is high, the hydrolysis rate is low and thus large particles are formed. The hydrolysis reaction of alkoxide with acid often forms a monolithic gel [10-19]. On the other hand, the hydrolysis reaction with a base causes particle precipitation [20, 21].

It has been well noted that monosized spherical powders as ideal sinterable powders may be prepared by the controlled hydrolysis of metal alkoxide [22-30]. In addition, the alkoxide route enables high purity and uniform component powder to be obtained on the molecular level at lower temperature. Generally, monosized oxide powders were prepared by the controlled hydrolysis and condensation of metal alkoxide in the dilute alcohol solution. The precipitation factors such as a reactant concentration, a concentration ratio of alkoxide and water, temperature and ageing conditions had an effect on the particle

size, size distribution, morphology and state of agglomeration. The induction period for nucleation is very short with increasing either reactant concentration or ratio of alkoxide and water. However, monosized oxide powders through an alkoxide route were produced by a batch precipitation technique on a litre scale, in which the hydrolysis was carried out using a beaker and a magnetic mixer under the nitrogen atmosphere. The batch process is not large enough to obtain many monosized colloidal particles. So far, several types of continuous reactor systems have been designed [31-34].

Ring and co-workers [31,32] have indicated several problems in the batch process: (1) high operating cost, (2) low productivity and (3) batch-to-batch product variation. They have developed continuous precipitation of monosized TiO_2 powders with a packed bed crystallizer and static mixer reactor. Van Zyl *et al.* [33] synthesized TiO_2 and ZrO_2 powders by the hydrolysis of alkoxide using a stirred tank reactor with a glass static mixer. However, these reactor systems have several problems in the preparation of monosized powders. (1) The nucleation model is governed by a multi-point nucleation model in the reactor with a packed bed or a static mixer. The particle size distribution is broader than that of particles formed by a single-point nucleation model. (2) Unreacted alkoxide is absorbed on the glass beads as an impurity in a packed bed. (3) A dispersant, such as hydroxy-propyl-cellulose (HPC), must be used to prevent agglomeration during particle growth [35-38]. HPC is effective for the preparation of nonagglomerated powders, but it is difficult to control the particle size by an addition of HPC.

Kalley and Fisher [39] and Matijević and Hsu [40] designed another type of reactor system in which monodispersed colloidal metal oxide particles were formed by a continuous forced hydrolysis of metal salts solution at elevated temperature. This continuous process has low productivity for the preparation of monosized powders. However, the design of this process was useful for the development of our continuous system in which the alkoxide-alcohol solution was aged at elevated temperature.

The objectives of this work were as follows. (1) The development of a mixer applicable to the single-point nucleation model. (2) Confirmation of reproducibility and reliability in the preparation of monosized powders by long-term production. (3) Preparation of several types of monosized colloidal particles.

This paper describes the preparation and characterization of monosized colloidal particles by a modified continuous reactor system, in which the hydrolysis and condensation of metal alkoxide continuously and rapidly proceeds in an alcohol solution.

2. Experimental procedure

2.1. Materials

The metal alkoxides used as reactant solutions were zirconium butoxide ($Zr(OC_4H_9)_4$), titanium ethoxide ($Ti(OC_2H_5)_4$), silicon ethoxide ($Si(OC_2H_5)_4$), yttrium isopropoxide ($Y(iso-OC_3H_7)_3$), and tantalum butoxide ($Ta(OC_4H_9)_5$). Triply distilled and deionized water was used; 200 proof ethanol was used as a solvent and the water present in it was reduced to 50 p.p.m. using molecular sieves 3A (1/16). The metal alkoxides were used without further purification.

2.2. Continuous hydrolysis of the alkoxide

A schematic diagram of the continuous reactor system which we have developed is presented in Fig. 1. This system is modified from an apparatus which we developed in 1989 [34]. The apparatus consisted of four sections: (1) a glove box to enclose the two reactant solutions and product slurry under conditions of low humidity and a temperature maintained at 25 °C, (2) a peristaltic pump to supply the two reagents at equal flow rates, (3) an electromagnetic stirrer for hydrolysis, and (4) a 300 m long vinyl chloride tube of 4 mm i.d. for solution ageing. This was wound on a cylinder and heated at 50 °C in the thermostatted box, in which the ageing temperature was controlled by an air heater with a sensor. Alkoxide-ethanol solution and water-ethanol solutions were introduced into an electromagnetic stirrer and uniform mixing was carried out at constant time. The hydrolysis reaction rapidly occurred, followed by turbidity as the particle precipitate appeared. The cloudy solution was passed through an ageing tube for 40 min and the degree of turbidity increased with ageing time. This indicated that the particles had grown to sub-micrometre size. After the ageing had finished, the particles formed were separated from the powder suspension using the centrifugal separator at 4500 r.p.m. for 5 min and then dried at 200 °C for 24 h. The reac-

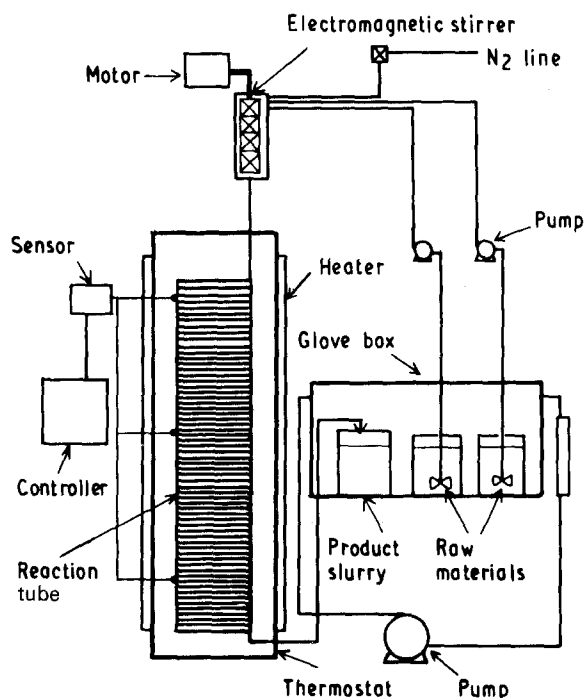


Figure 1 Schematic illustration of the continuous reactor system.

tion parameters for powder preparation are listed in Table I.

2.3. Characterization of monosized oxide powders

The determination of particle size, particle size distribution and morphology was made using scanning electron microscopy (Hitachi Model S800). The assessment of particle size distribution and the state of agglomeration were made by image analysis of transmission (Jeol Model JSM 200B) and scanning electron micrographs. 300 particles were measured for each sample. The thermal behaviour of as-prepared powders was observed by thermogravimetric (TG) (Rigaku Model TGD-7000) and differential thermal analysis (DTA) (Rigaku Model TGD-7000) in an air atmosphere at a heating rate of 10 °C min⁻¹. Crystalline phases were determined by powder X-ray diffraction (Jeol Model JRX-30VA).

3. Results and discussion

In a batch process, the requirement for the preparation of monosized powders is a short nucleation

TABLE I Reaction parameters for powder preparation

Parameter	Conditions
Concentration (mol l ⁻¹)	
Metal alkoxide	0.05–1.0
Water	0.05–1.0
^a Water/NH ₃	7.5/2.5
Temperature (°C)	25–70
Reaction time (min)	30–300
Mixing rate (r.p.m.)	60–360
Flow rate (cm ³ l ⁻¹)	30–65

^a Silica

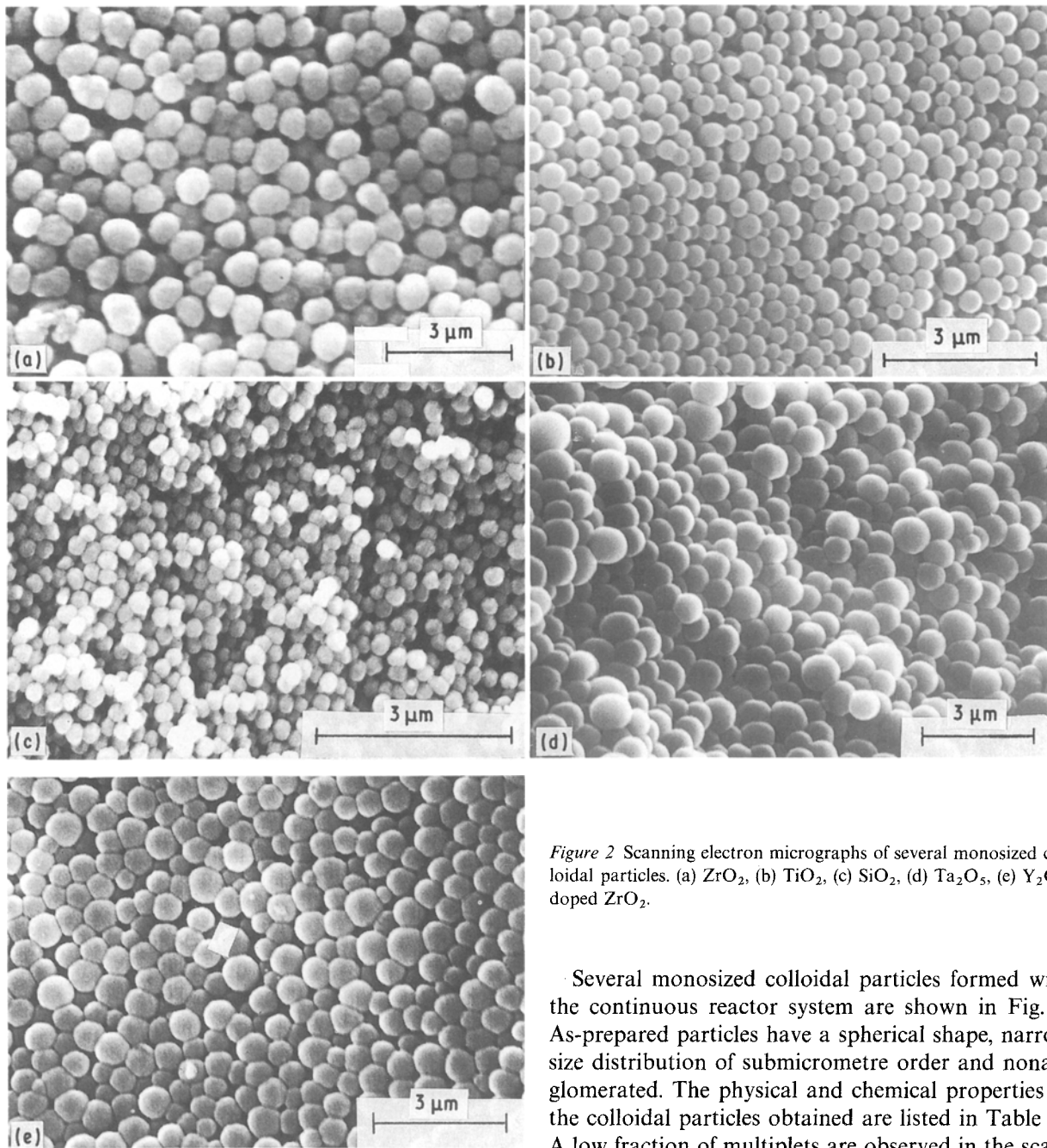


Figure 2 Scanning electron micrographs of several monosized colloidal particles. (a) ZrO_2 , (b) TiO_2 , (c) SiO_2 , (d) Ta_2O_5 , (e) Y_2O_3 -doped ZrO_2 .

Several monosized colloidal particles formed with the continuous reactor system are shown in Fig. 2. As-prepared particles have a spherical shape, narrow size distribution of submicrometre order and nonagglomerated. The physical and chemical properties of the colloidal particles obtained are listed in Table II. A low fraction of multiplets are observed in the scanning electron micrographs, but the monosized colloidal particles obtained are comparable to those that are synthesized in a batch process.

period, which produces a homogeneous nucleation and growth throughout the solution. Barringer and Bowen [41] proposed several conditions to be successful in the synthesis of monosized oxide powders from metal alkoxide: (1) proper reagent concentration and molar ratio of alkoxide to water are necessary to promote homogeneous nucleation; (2) reagents must be completely mixed before nucleation; (3) insoluble impurities must be removed from the reagent to prevent heterogeneous nucleation; (4) the colloid stability in the solution is maintained during the initial reaction stage by employing repulsive steric or electrostatic forces. However, particles with a diameter of less than $0.1 \mu m$ flocculated on collision in the neutral solution. The above conditions must also be satisfied in the continuous reactor system.

3.1. Effect of reagent concentration

Typical ZrO_2 particles, which are formed at 40 min ageing under conditions of various reagent concentrations are shown in Fig. 3. The concentration range of alkoxide and water, in which monosized ZrO_2 particles are formed, is shown in Fig. 4. In the 40 min ageing test, monosized ZrO_2 particles were precipitated under the conditions of 0.05 – 0.2 and 0.2 – $0.5 \text{ mol l}^{-1} H_2O$. An optimum concentration range was existed in the preparation of other monosized powders such as TiO_2 , Y_2O_3 -doped ZrO_2 and Ta_2O_5 , but an optimum molar ratio of water and alkoxide did not exist when the alkoxide concentration was more than 0.3 mol l^{-1} . The optimum conditions varied with increasing ageing period, but the deviation was slight. ZrO_2 particles were spherical

TABLE II Physical and chemical properties of as-prepared powders

	ZrO ₂	TiO ₂	Ta ₂ O ₅	SiO ₂	Y ₂ O ₃ -ZrO ₂
Precursor	Zr(OBu) ₄	Ti(OEt) ₄	Ta(OBu) ₅	Si(OEt) ₄	Zr(OBu) ₄ Y(iso-OPr) ₃
Shape	Spherical	Spherical	Spherical	Spherical	Spherical
Size (μm)	0.64	0.54	0.84	0.32	0.67
σ _g	1.08	1.06	1.10	1.08	1.10
Crystal form	Amorphous ↓ 1000 °C monoclinic	Amorphous ↓ 400 °C anatase ↓ 800 °C rutile	Amorphous ↓ 740 °C β-Ta ₂ O ₅	Amorphous ↓ 1000 °C amorphous	Amorphous ↓ 1000 °C monoclinic
State of agglomeration	Unagglomerated	Unagglomerated	Unagglomerated	Unagglomerated	Unagglomerated
Yield (%)	60	70	73	58	67
Volatile (%)	10	12	18	8	14
Surface area (m ² g ⁻¹)	10	10	12	20	11
Shrinkage (%)	20	24	31	15	24

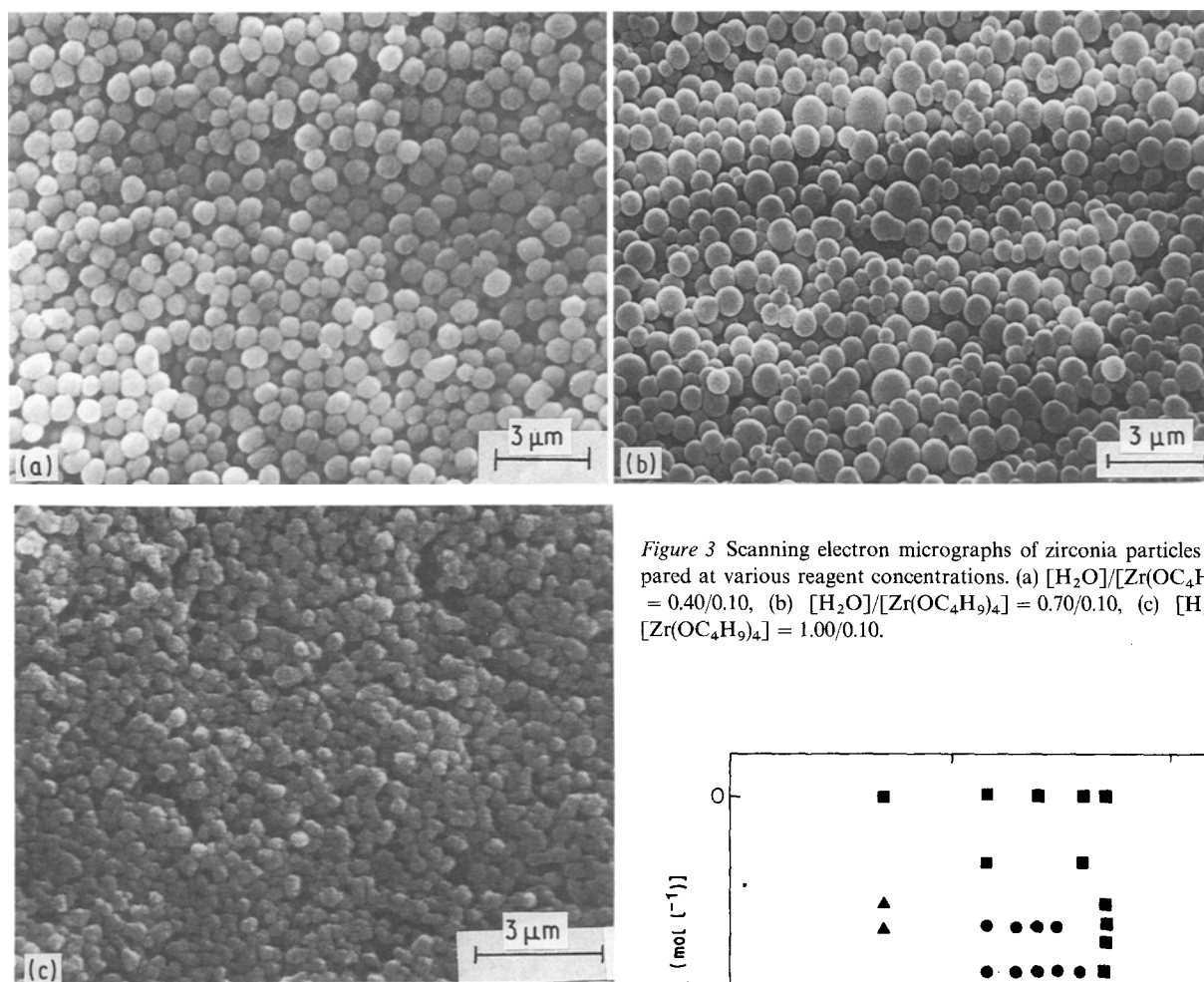


Figure 3 Scanning electron micrographs of zirconia particles prepared at various reagent concentrations. (a) [H₂O]/[Zr(OC₄H₉)₄] = 0.40/0.10, (b) [H₂O]/[Zr(OC₄H₉)₄] = 0.70/0.10, (c) [H₂O]/[Zr(OC₄H₉)₄] = 1.00/0.10.

with a diameter of 0.1–0.8 μm and their geometrical standard deviation, σ_g, was less than 1.2 from TEM and SEM image analysis. The fractions of singlets on the top and fracture surface from scanning electron micrographs were 90% and 75%, respectively. The particle size and yield increased with increasing concentration of alkoxide, as shown in Figs 5 and 6. However, when the metal alkoxide was hydrolysed at

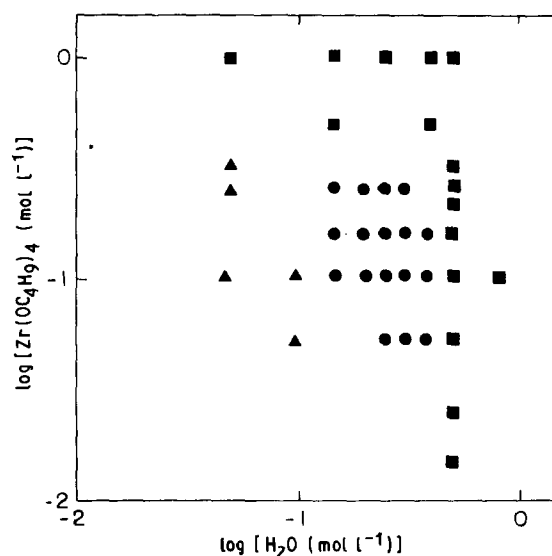


Figure 4 Formation of zirconia particles with various reagent concentrations. (●) Monosized, (▲) bimodal, (■) agglomerates.

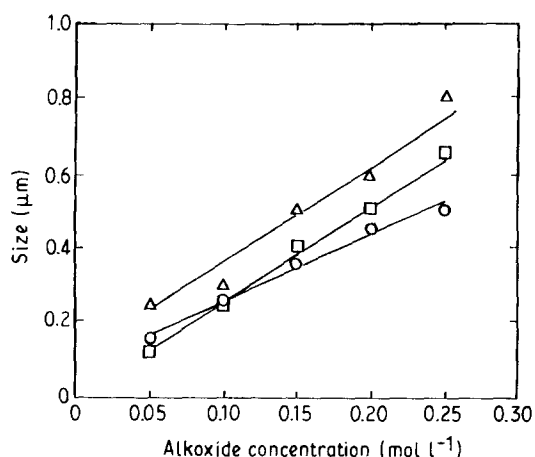


Figure 5 Particle size as a function of alkoxide concentration. (Δ) Ta_2O_5 , (\square) ZrO_2 , (\circ) TiO_2 . Water concentration 0.3 mol l^{-1} , reaction time 90 min.

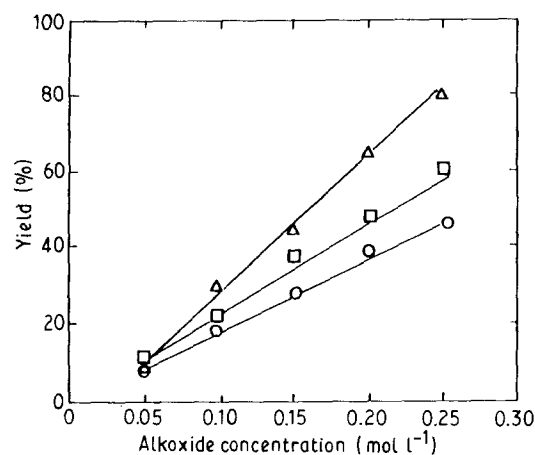
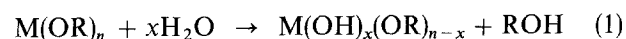


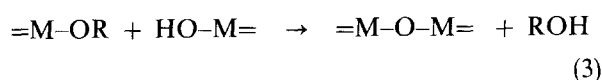
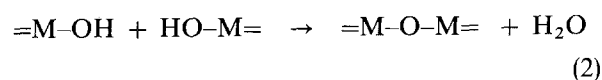
Figure 6 Yield as a function of alkoxide concentration. (Δ) Ta_2O_5 , (\square) ZrO_2 , (\circ) TiO_2 . Water concentration 0.3 mol l^{-1} , reaction time 90 min.

more than 1.0 mol l^{-1} water, the particle size and fraction of singlets were decreased. The fraction of singlets on the top and fracture surface was 30% and 15%, respectively. Moreover, gelation occurred at more than 10 mol l^{-1} water. Similarly, agglomerated and irregularly shaped particles, such as doublets and triplets, were largely formed, as the concentration of alkoxide was increased to more than 0.3 mol l^{-1} .

The overall reaction on the formation of oxide particles consists of hydrolysis of metal alkoxide and condensation of the hydrolysis species. The hydrolysis is given by Reaction 1; the hydrolysis species generated may differ with the hydrolysis conditions used.



This undergoes condensation to produce the polymer



Condensation proceeds either through water elimination (Reaction 2) or alcohol elimination (Reaction 3). The above two condensations may occur simultan-

ously. In the reactor system, the particles grew with increasing reagent concentration, but they did not grow or gelate when the reagent concentration was above 0.7 and 0.3 mol l^{-1} for water and alkoxide, respectively. In the formation of monosized powders, these results suggest that the homogeneous nucleation and growth are dependent on the proper reagent concentration and not the molar ratio of water and alkoxide. When the proper reagent concentration is not satisfied, two phenomena occur: (1) formation of multiplets, such as agglomeration and aggregation, due to the many nuclei derived from the rapid nucleation and growth, in which the hydrolysis and condensation rate are not controlled; (2) no particle formation due to the precipitation period being longer than the ageing time, at which the concentration of the hydrolysis species is always lower than the critical concentration during ageing.

3.2. Effect of ageing temperature and time

Fig. 7 shows the influence of ageing temperature on particle characteristics such as size, size distribution, morphology and state of agglomeration. The particle size and yield slightly increased with increasing ageing temperature. The geometrical standard deviation was less than 1.2 in all experiments. However, particle morphology and the state of agglomeration were affected by temperature as shown in Fig. 8. Agglomerated and irregular particles were formed when ageing was carried out at a temperature above 60°C . This suggests that the colloidal particles generated are strongly agglomerated by vigorous Brownian motion between them in the solution. To obtain monosized colloidal particles, the reaction must be performed at a temperature below 50°C . In this reactor system, the ageing time is a means of controlling the particle size. Fig. 9 shows the change of particle size as a function of reaction time: the particle size increased with ageing time. However, particles greater than $1.0 \mu\text{m}$ were not obtained after 300 min ageing. This result suggested that no alkoxide in the mother liquid remained after

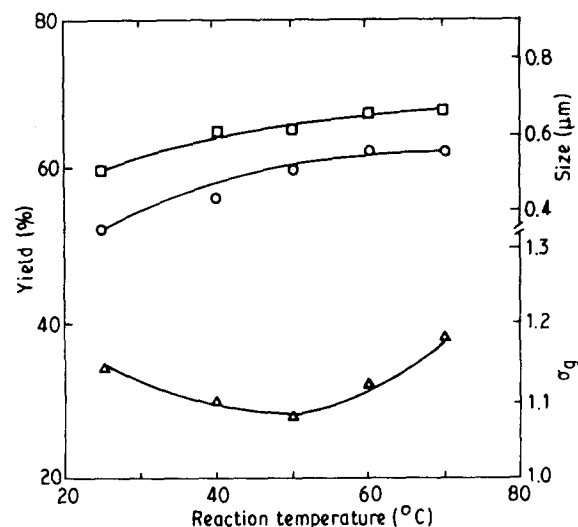


Figure 7 Particle characteristics as a function of ageing temperature. Concentrations: $\text{Zr}(\text{OC}_4\text{H}_9)_4$ 0.15 mol l^{-1} , water 0.30 mol l^{-1} . Reaction time 90 min. (\circ) yield, (\square) size, (Δ) σ_g .

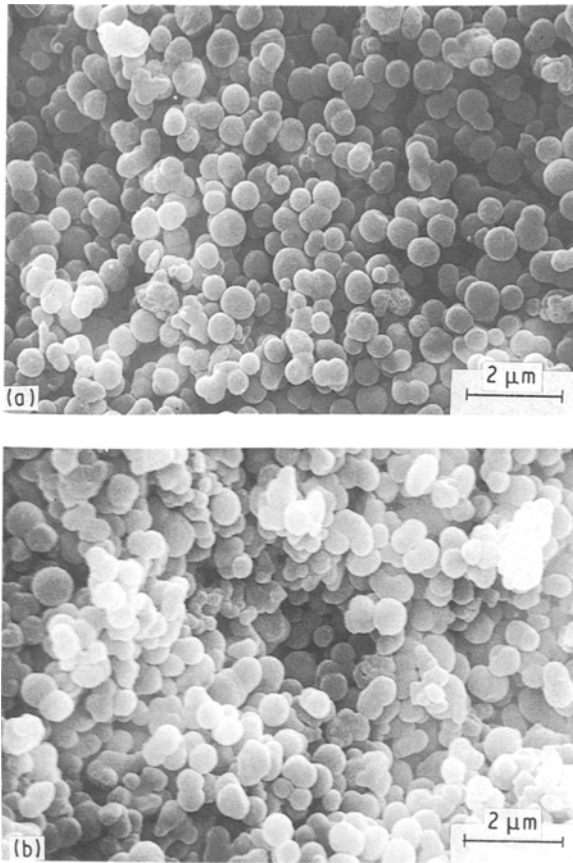


Figure 8 Variation in morphology of zirconia particles with ageing temperature: (a) 60°C, (b) 80°C.

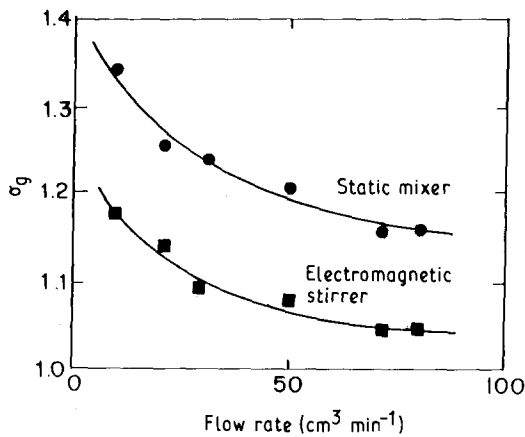


Figure 9. Geometrical standard deviation as a function of flow rate.

300 min ageing. For particle growth to occur, the polymeric species must be supplied to the particle surface.

3.3. Effect of mixing

In dispersion models [31, 32] for non-ideal flow in the packed-bed reactor filled with glass beads and the static mixer reactor, the multipoint nucleation model was applied. The resultant particles have a larger geometrical standard deviation of particle size. It is necessary to develop the mixer such that the nucleation approximates the ideal single-point nucleation model. Fig. 10 shows the effect of particle size distribution

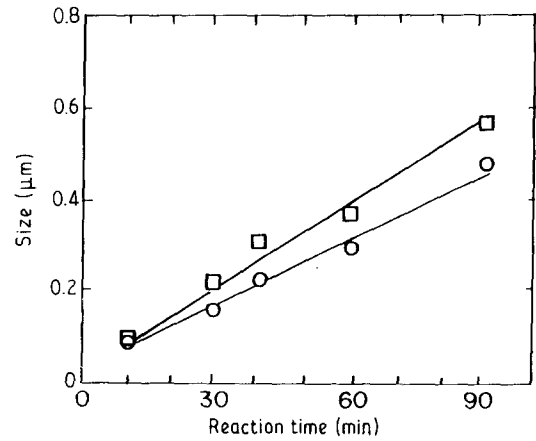


Figure 10. Particle size as a function of reaction time. (□) ZrO₂, (○) TiO₂. Alkoxide concentration 0.2 mol l⁻¹, water concentration 0.3 mol l⁻¹.

on two types of mixer, a 25 cm Teflon static mixer and an electromagnetic stirrer, respectively. The smaller geometrical standard deviation of particle size was given by the use of an electromagnetic stirrer rather than a static mixer. The greater the flow rate of the reagent solution, the narrower was the particle size distribution.

3.4. Reliability and reproducibility of the continuous reactor system

A long-term powder production was performed to confirm the reliability and reproducibility of this reactor system for the preparation of monosized ceramic raw powders on an industrial scale. The hydrolysis and ageing process was continuously performed for 10 h. The resultant particle characteristics (such as size, size distribution and yield) of monosized zirconia powders are shown in Fig. 11 as a function of production time. In this reactor, 24 g dried powders were obtained per hour. The amount of powder can be increased by using a larger stirrer, wider ageing tube and a surfactant.

3.5. Morphology of particles obtained by crystallization

Monosized powders prepared in this reactor system cannot generally be used as ceramic raw materials,

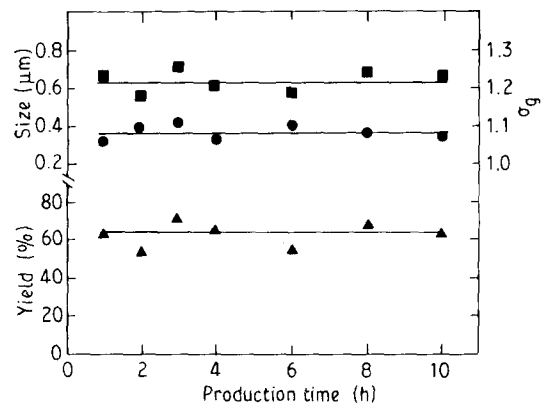


Figure 11 Particle characteristics as a function of production time. (■) Size, (●) σ_g, (▲) yield.

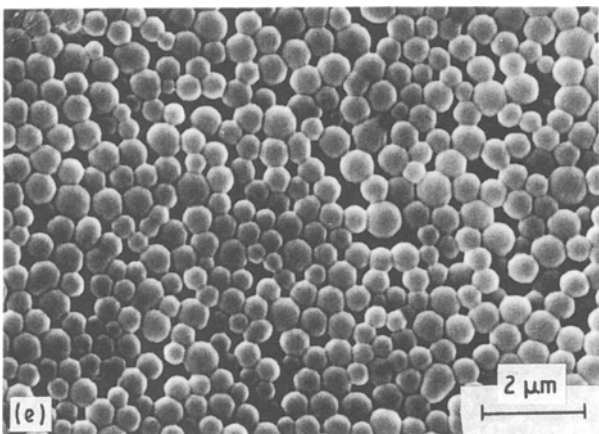
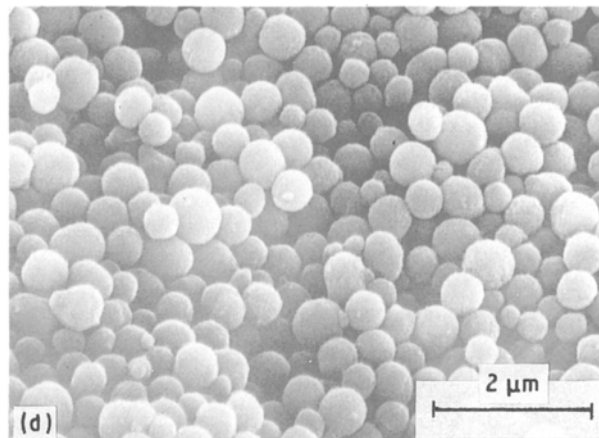
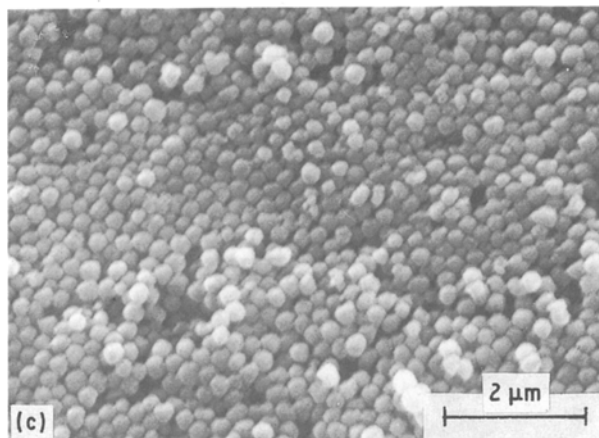
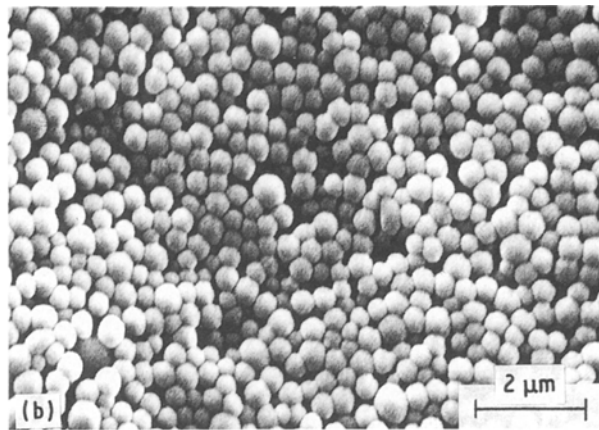
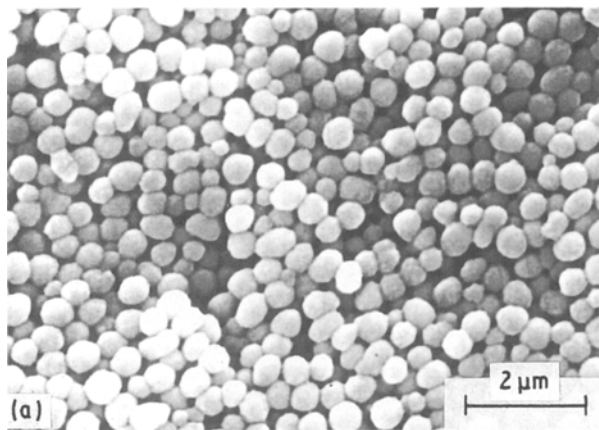


Figure 12 Morphology of particles obtained by calcination at 1000 °C. (a) ZrO_2 , (b) TiO_2 , (c) SiO_2 , (d) Ta_2O_5 , (e) Y_2O_3 -doped ZrO_2 .

because as-prepared powders are amorphous (from X-ray analysis) and residual hydroxy and alkoxy groups are absorbed on the particle surface (from DTA–TG analysis). The absorbed species are burned out up to 400 °C in all powders. Hence, they must be crystallized by calcination. Fig. 12 shows scanning electron micrographs of ZrO_2 , TiO_2 , Ta_2O_5 , SiO_2 , Y_2O_3 -doped ZrO_2 particles crystallized by calcination at 1000 °C for 2 h. After calcination, their particle size was decreased due to the dehydration and decomposition of organic species. Their particle morphology also remained spherical and unagglomerated. This confirmed that these powders could be used as ceramic raw materials.

4. Conclusion

A continuous reactor system, in which monosized oxide powders were prepared by the hydrolysis of metal alkoxide in a dilute alcohol solution, was designed. Monosized powders were only produced in a narrow concentration range of reactants (metal alkoxide and water). The reagent concentration had an effect on particle size, size distribution, morphology and state of agglomeration. Ageing temperature had an effect on particle morphology and state of agglomeration. The electromagnetic stirrer affected the formation of monosized powders in comparison with a static mixer. A narrow size distribution of powders was obtained by mixing with a greater flow rate and the particle size could be controlled to between 0.1 and 1.0 μm by varying the experimental parameters. The physical and chemical properties of monosized colloidal particles were comparable to those obtained using a batch process. Heating of the as-prepared sub-micrometre particles to 1000 °C resulted in a slight decrease of particle size. Particle morphology was retained after crystallization.

Acknowledgements

The authors thank Nippon Sheet Glass Foundation For Materials Science, The Japan Securities Scholarship Foundation, and The Hokuriku Industrial Advancement Center, for supporting the work.

References

1. K. S. MAZDIYASNI, *Ceram. Int.* **8** (1982) 42.
2. W. W. RHODES, *J. Amer. Ceram. Soc.* **64** (1981) 19.
3. M. F. YAN, *Chem. Engng Sci.* **48** (1981) 53.
4. K. KAMIYA, S. SAKKA and M. MIZUTANI, *J. Ceram. Soc. Jpn* **86** (1978).
5. M. D. SACKS and T. Y. TESNG, *J. Amer. Ceram. Soc.* **67** (1984) 532.
6. E. M. RABIONVICH, *J. Mater. Sci.* **20** (1985) 4259.
7. K. KAMIYA, K. TANIMOTO and T. YOKO, *J. Mater. Sci.* **5** (1986) 421.
8. N. TOHGE, A. MATSUDA and T. MINAMI, *J. Ceram. Soc. Jpn* **95** (1987) 182.
9. A. MATSUDA, Y. MATSUNO, S. KATAYAMA and T. TSUNO, *J. Mater. Sci. Lett.* **8** (1989) 902.
10. B. E. YOLDAS, *J. Mater. Sci.* **21** (1986) 1080.
11. *Idem.*, *ibid.* **21** (1986) 1087.
12. *Idem.*, *ibid.* **12** (1977) 1203.
13. *Idem.*, *ibid.* **14** (1979) 1843.
14. K. C. SONG and I. J. CHUNG, *J. Non-Cryst. Solids* **108** (1989) 37.
15. A. C. PIERRE and D. R. UHLMANN, *J. Amer. Ceram. Soc.* **70** (1987) 28.
16. J. Y. CHANE CHING and L. C. KLEIN, *ibid.* **71** (1988) 83.
17. *Idem.*, *ibid.* **71** (1988) 86.
18. B. E. YOLDAS, *J. Appl. Chem. Biotechnol.* **23** (1973) 803.
19. *Idem.*, *Amer. Ceram. Soc. Bull.* **54** (1975) 289.
20. W. STÖBER, A. FINK and E. BOHN, *J. Colloid Interface Sci.* **26** (1968) 62.
21. T. SHIMOHIRA and H. ISHIJIMA, *J. Chem. Soc. Jpn* **9** (1981) 1503.
22. T. IKEMOTO, K. UEMATSU, N. MIZUTANI and M. KATO, *J. Ceram. Soc. Jpn* **93** (1985) 261.
23. E. A. BARRINGER and H. K. BOWEN, *Langmuir* **1** (1985) 414.
24. J. H. JEAN and T. A. RING, *ibid.* **2** (1986) 251.
25. B. FEGLEY, P. WHITE and H. K. BOWEN, *Amer. Ceram. Soc. Bull.* **64** (1985) 1115.
26. T. OGIHARA, N. MIZUTANI and M. KATO, *Ceram. Int.* **13** (1987) 35.
27. K. UCHIYAMA, T. OGIHARA, T. IKEMOTO, N. MIZUTANI and M. KATO, *J. Mater. Sci.* **22** (1987) 4343.
28. R. H. HEISTAND and Y. H. CHIA, *Mater. Res. Soc. Symp. Proc.* **73** (1986) 92.
29. T. OGIHARA, T. IKEMOTO, N. MIZUTANI, M. KATO and Y. MITARAI, *J. Mater. Sci.* **21** (1986) 2771.
30. T. OGIHARA, H. KANEKO, N. MIZUTANI and M. KATO, *J. Mater. Sci. Lett.* **7** (1988) 867.
31. T. A. RING, *Chem. Engng Sci.* **39** (1984) 1731.
32. J. H. JEAN, D. M. GOY and T. A. RING, *Amer. Ceram. Soc. Bull.* **66** (1987) 1517.
33. A. van ZYL, P. M. SMITH and A. I. KINGDON, *Mater. Sci. Engng* **78** (1986) 217.
34. T. OGIHARA, M. IKEDA, M. KATO and N. MIZUTANI, *J. Amer. Ceram. Soc.* **72** (1989) 1598.
35. J. H. JEAN and T. A. RING, *Amer. Ceram. Soc. Bull.* **65** (1986) 1574.
36. *Idem.*, *Mater. Res. Soc. Symp. Proc.* **73** (1986) 85.
37. T. E. MATES and T. A. RING, *Colloid Surf.* **24** (1987) 299.
38. J. H. JEAN and T. A. RING, *ibid.* **29** (1988) 273.
39. N. KALLEY and I. FISCHER, *ibid.* **13** (1985) 145.
40. E. MATIJEVIĆ and W. P. HSU, *J. Colloid Interface Sci.* **118** (1987) 506.
41. E. A. BARRINGER and H. K. BOWEN, *J. Amer. Ceram. Soc.* **65** (1982) C-199.

Received 21 November 1990
and accepted 24 January 1991